

Diffuse MeV Gamma-rays and Galactic 511 keV Line from Decaying WIMP Dark Matter

Jose A. R. Cembranos¹ and Louis E. Strigari²

¹ *William I. Fine Theoretical Physics Institute,
University of Minnesota, Minneapolis, 55455, USA*

² *Department of Physics and Astronomy,
University of California, Irvine, CA 92697, USA*

Abstract

The origin of both the diffuse high-latitude MeV gamma-ray emission and the 511 keV line flux from the Galactic bulge are uncertain. Previous studies have invoked dark matter physics to independently explain these observations, though as yet none has been able to explain both of these emissions within the well-motivated framework of Weakly-Interacting Massive Particles (WIMPs). Here we use an unstable WIMP dark matter model to show that it is in fact possible to simultaneously reconcile both of these observations, and in the process show a remarkable coincidence: decaying dark matter with MeV mass splittings can explain both observations if positrons and photons are produced with similar branching fractions. We illustrate this idea with an unstable branon, which is a standard WIMP dark matter candidate appearing in brane world models with large extra dimensions. We show that because branons decay via three-body final states, they are additionally unconstrained by searches for Galactic MeV gamma-ray lines. As a result, such unstable long-lifetime dark matter particles provide novel and distinct signatures that can be tested by future observations of MeV gamma-rays.

PACS numbers: 95.35.+d, 11.10.Kk, 12.60.-i, 98.80.Cq

I. INTRODUCTION

The existence of dark matter is well-established, yet its identity remains elusive. Standard dark matter candidates include Weakly-Interacting Massive Particles (WIMPs), which have mass $\sim 0.1 - 1$ TeV, and arise from independent attempts in particle physics to understand the mechanism of electroweak symmetry breaking. Well-studied signatures of WIMPs include elastic scattering off nucleons in underground laboratories, missing energy signals at colliders, and particle production via self-annihilation in Galactic and extragalactic sources (e.g. [1, 2, 3, 4, 5]).

These standard signatures, however, do not provide the only means to test the properties of dark matter. As an additional example, one may also consider invoking dark matter physics to explain anomalous signatures in observed photon or cosmic ray emission spectra, even at energies seemingly far removed from those associated with weak-scale physics. In fact, in recent years, dark matter models have been constructed to explain astrophysical particle production over a variety of energy scales: these include ultra-high energy cosmic rays [6], 511 keV line emission from the Galactic bulge [7, 8, 9, 10, 11, 12, 13], or the diffuse MeV gamma-ray background [14, 15]. Though of course all of these anomalies will not be due to exotic dark matter physics, the observed emissions can provide strong constraints on well-motivated dark matter models, and further they may help identify the interesting regions of parameter space for a given dark matter model.

In this paper we focus on two of the aforementioned anomalies: the diffuse MeV gamma-ray background and the 511 keV line flux from the Galactic bulge. As we discuss below, known “astrophysical” sources have both spectral shapes and rates that are unable to account for these observed emissions. The lack of well-motivated sources, as well as the similarities of energy scales, has given rise to speculation that both of these anomalies can be explained within the context of a single dark matter model [16], albeit at the cost of abandoning the well-motivated WIMP framework. Remaining within the confines of WIMP models, these emissions have been separately reconciled by invoking unstable WIMPs with nearly degenerate, \sim MeV scale mass splittings: the 511 keV line flux has been studied in Refs. [12, 13], and the diffuse MeV photon background has been studied in Refs. [17, 18]. The goal of this paper is to show that, remarkably, *both* the 511 keV line emission and the diffuse MeV gamma-ray spectrum can be explained in the context of a decaying WIMP model, characterized by a lifetime of 10^{20} s and near equal branching fraction to photons and electrons.

Generically, we focus on a scenario in which the WIMP mass spectrum is highly degenerate, characterized by \sim MeV mass splittings between the next-to-lightest particle (NLP) and lightest particle (LP). Both WIMPs freeze out under the standard conditions in the early Universe, and one of them is unstable with a lifetime in excess of the Hubble time. The NLP decays to three-body final states such as $\text{NLP} \rightarrow \text{LP} + \gamma + \gamma$, $\text{NLP} \rightarrow \text{LP} + e^+ + e^-$, $\text{NLP} \rightarrow \text{LP} + \bar{\nu} + \nu$. Two-body decays are assumed to be either highly suppressed or forbidden. Phenomenological consequences of two-body decays with similar lifetimes, and implications for the diffuse MeV photon background, were introduced in Ref. [17], and further discussed in Ref. [19]. Additionally, prospects for detecting long-lifetime decaying dark matter with the GeV gamma-ray background were considered in Ref. [20].

As a specific implementation of the above idea, we consider the brane world scenario (BWS), which has become one of the most popular extensions to the Standard Model (SM). In the BWS, particles are confined to live on a three-dimensional brane embedded in a higher

dimensional ($D = 4 + N$) space-time, while the gravitational interaction has access to the entire bulk space. The fundamental scale of gravity in D dimensions, M_D , can be lower than the Planck scale, M_P . In the original proposal [21, 22], the main aim was to address the hierarchy problem, and for that reason the value of M_D was taken to be around the electroweak scale. However, brane cosmology models have also been proposed in which M_D is much larger than the TeV scale [23, 24]. In this paper, we consider a general BWS with arbitrary fundamental scale M_D ; since we neglect gravitational effects, our results do not depend on this scale once sufficiently high.

In general, the existence of extra dimensions is responsible for the appearance of new fields on the brane. On one hand, we have the tower of Kaluza-Klein (KK) modes of fields propagating in the bulk space, i.e. the gravitons. On the other, since the brane has a finite tension, f^4 , its fluctuations will be parametrized by π^α fields called branons. When translational invariance in the bulk space is an exact symmetry, these fields can be understood as the massless Goldstone bosons arising from the spontaneous breaking of that symmetry induced by the presence of the brane [25, 26]. However, in the most general case, translational invariance will be explicitly broken and therefore we expect branons to be massive fields. When branons are properly taken into account, the coupling of the SM particles to any bulk field is exponentially suppressed by a factor $\exp[-M_{KK}^2 M_D^2 / (8\pi^2 f^4)]$, where M_{KK} is the mass of the corresponding KK mode [27, 28]. As a consequence, if $f \ll M_D$, the KK modes decouple from the SM particles. Therefore, for flexible enough branes, the only relevant degrees of freedom at low energies in the BWS are the SM particles and branons.

The potential signatures of branons at colliders have been considered in Refs. [29, 30, 31], and astrophysical and cosmological implications have been studied in Refs. [31, 32]. Moreover in Ref. [33] the possibility that massive branons could account for the observed dark matter of the Universe was studied in detail (see also [31]). Here, for the first time, we consider branon phenomenology with MeV mass splittings and lifetimes in excess of the age of the Universe. Due to their universal coupling to the SM, decays of unstable branons produce electrons and photons at the same rate in decays, leading to the aforementioned consequences for diffuse MeV gamma-rays and the 511 keV line flux.

This paper is organized as follows. In section II, we review the observations of the cosmic and Galactic gamma-ray backgrounds and the 511 keV signal. Section III we summarize the salient features of the brane world model, and in section IV we present the resulting astrophysical signatures. Finally, in sections V and VI we discuss other possible signatures and recap our main conclusions.

II. GAMMA-RAY OBSERVATIONS

In this section, we introduce and discuss the gamma-ray emission spectra we will analyze within the framework of decaying dark matter. We focus on two specific observations: the 511 keV photon line flux from the Galactic center and the high latitude isotropic diffuse MeV photon emission. We also, for completeness, discuss the diffuse MeV gamma-ray emission from the Galactic center: in the discussion section below we show how these observations pertain to our model constraints.

A. 511 keV line flux from the Galactic center

The SPI spectrometer on the INTEGRAL (International Gamma-ray Astrophysics Laboratory) satellite has measured a 511 keV line emission of $1.05 \pm 0.06 \times 10^{-3}$ photons $\text{cm}^{-2} \text{s}^{-1}$ from the Galactic bulge [34], confirming earlier measurements [35]. The emission region is observed to be approximately spherically-symmetric about the Galactic bulge, with a full width half maximum (FWHM) $\sim 8^\circ$. There is a very low level detection from the Galactic disk, $\sim 4\sigma$, compared to the 50σ detection from the bulge. The 511 keV line flux is consistent with an e^+e^- annihilation spectrum, fit by the sum of three distinct components: a narrow and broad line flux, both centered at 511 keV, and a continuum spectrum extending to energies less than 511 keV. The narrow line flux arises both from the direct annihilation of thermalized positrons into two photons or through para-positronium formation primarily in the cold and warm phase of the inter-stellar medium (ISM). The broad line flux, which has a width of 5.4 ± 1.2 keV FWHM, arises from the annihilation of para-positronium in flight in the warm and neutral phase of the ISM. The < 511 keV continuum emission arises from the annihilations in the ortho-positronium state. The number of 511 keV gamma-rays produced per positron is $2(1 - 3p/4)$, where p is the positronium fraction [36]. By detailed fitting of the spectrum to annihilation in different phases of the ISM, Ref. [37] concludes that $p = 0.935_{-1.6}^{+0.3}$. A model independent fitting of the spectra to a broad line, narrow line, continuum spectra, and Galactic diffuse component concludes that $p = 0.967 \pm 0.022$. A precise determination of the positronium fraction thus ultimately depends on both the nature of the source of the positrons as well as the temperature of the medium in which they annihilate.

The source of the Galactic positrons is uncertain. The fact that the annihilation takes place primarily in the warm neutral and warm ionized medium implies that the sources of the positrons are diffusely distributed, and that the initial kinetic energy of the positrons is less than a few MeV [36, 38]. The sources of the positrons are likely contained within the observed emission region; the propagation distance from creation to annihilation is at most of order ~ 100 pc. Type Ia supernovae (SNIa) are a candidate for the source of positrons, however recent estimates of the escape fraction of positrons from SNIa indicate that they cannot account for the entire 511 keV emission [39]. Several other astrophysical sources have been proposed [40, 41, 42], however none of these sources seem adequate to produce the intensity and spatial distribution of the observed line flux.

B. Isotropic diffuse MeV gamma-ray background at high Galactic latitude

COMPTEL (the Compton Imaging Telescope) and SMM (the Solar Maximum Mission) have measured an isotropic gamma-ray background at high Galactic latitudes ($\gtrsim 10^\circ$) over the energy ranges 0.8–30 MeV [43] and 0.3–7 MeV [44], respectively. More recently, INTEGRAL has measured a diffuse photon background over the energy range 5–100 keV [45]. We follow the notation of Ref. [19] and refer to these backgrounds as the isotropic diffuse photon background (iDPB), as it may include contributions from both Galactic and extragalactic sources. At \sim MeV energies, the iDPB analysis is hindered by instrumental and cosmic-ray backgrounds, which must be carefully subtracted to reveal the underlying signal. Over the COMPTEL and SMM energy ranges, which will be important for our analysis below, the observed spectrum is observed to fall like a power law, with $dN/dE \sim E^{-2.4}$ [43].

Below energies of a few hundred keV, normal active galactic nuclei (AGN) are able to

explain the mean flux of the cosmic X-ray background [46]. A rare population of beamed AGN, or blazars, provide an important contribution to the iDPB for energies $\gtrsim 10$ MeV [47], though there is still room for other sources at these energies [48]. The iDPB is observed to smoothly transition in between these two energies, however, in the range $1 \text{ MeV} \lesssim E_\gamma \lesssim 5 \text{ MeV}$, no astrophysical source can account for the observed iDPB. Blazars are observed to have a spectral cut-off ~ 10 MeV, and also only a few objects have been detected below this energy [49]. SNIa contribute below ~ 5 MeV, but they also cannot account for the entire spectrum [50, 51]. Recent modeling shows that nonthermal relativistic electrons which alter the AGN spectra for energies $\gtrsim 1$ MeV may account for this excess emission, though a detailed understanding of the iDPB at all energies $\gtrsim 1$ MeV will require matching the mean flux and the angular distribution of the sources [52].

C. Diffuse MeV gamma-rays from the Galactic center

COMPTEL has determined the flux spectrum of diffuse gamma-rays from the Galactic center region over the energy regime $1 - 20$ MeV [53]. These fluxes have been averaged over a latitude of $|l| < 30^\circ$ and longitude $|b| < 5^\circ$, with high latitudes being used to define the zero flux level. It is currently unclear whether the $1 - 20$ MeV spectrum is a result of diffuse or point source emission. For energies $\gtrsim 100$ MeV, the gamma-ray spectrum is likely produced by both nucleon interactions with interstellar gas via neutral pion production and electrons via inverse compton scattering. For energies $\lesssim 100$ keV, point sources dominate the gamma-ray spectrum [54]. However, an inverse compton spectrum that matches the diffuse gamma-ray spectrum at ~ 100 MeV can account for at most 50% of the emission between $1 - 20$ MeV [55].

In addition to the diffuse measurement from COMPTEL, INTEGRAL has performed a search for gamma-ray lines originating within 13° from the Galactic center. Two lines were recovered: the aforementioned line at 511 keV and an additional line at 1809 keV. The 1809 keV line originates from the hydrostatic nucleosynthesis of radioactive elements in the cores of massive stars, where long-lived isotopes such as ^{26}Al are carried to the ISM, after which they subsequently decay mono-energetically. The 1809 keV line flux has been detected by INTEGRAL at a level of $\sim 10^{-4} \text{ cm}^{-2} \text{ s}^{-1}$. Other than these two gamma-ray lines, no other lines were detected up to upper flux limits of 10^{-5} - $10^{-2} \text{ cm}^{-2} \text{ s}^{-1}$, depending on line width, energy, and exposure.

III. BRANON PHENOMENOLOGY

Having introduced and discussed the gamma-ray emission spectra we consider, in this section we will briefly review the main properties of massive brane fluctuations (see Refs. [26, 30, 56] for a more detailed description). Focusing in particular on models that produce the observed abundance of dark matter, we present the formulae for determining the decay widths of long-lifetime branons to photons, electrons, and neutrinos.

A. Branon overview

We consider a typical brane model in large extra dimensions. The four-dimensional space-time, M_4 , is embedded in a D -dimensional bulk space which, for simplicity, it is assumed to

factorize as $M_D = M_4 \times B$. The extra space B is a given N -dimensional compact manifold, so that $D = 4 + N$. The brane lies along M_4 and we neglect its contribution to the bulk gravitational field. The bulk space M_D is endowed with a metric tensor G_{MN} , which we will assume for simplicity is given by

$$G_{MN} = \begin{pmatrix} \tilde{g}_{\mu\nu}(x, y) & 0 \\ 0 & -\tilde{g}'_{mn}(y) \end{pmatrix}. \quad (1)$$

The position of the brane in the bulk can be parametrized as $Y^M = (x^\mu, Y^m(x))$, with $M = 0, \dots, 3 + N$. We have chosen the bulk coordinates so that the first four are identified with the space-time brane coordinates x^μ . We assume the brane to be created at a certain point in B , $Y^m(x) = Y_0^m$, which corresponds to its ground state. We will also assume that B is a homogeneous space, so that brane fluctuations can be written in terms of properly normalized coordinates in the extra space: $\pi^\alpha(x) = f^2 Y^\alpha(x)$, $\alpha = 1, \dots, N$. The induced metric on the brane in its ground state is simply given by the four-dimensional components of the bulk space metric, i.e. $g_{\mu\nu} = \tilde{g}_{\mu\nu} = G_{\mu\nu}$. However, when brane excitations are present, the induced metric is given by

$$g_{\mu\nu} = \partial_\mu Y^M \partial_\nu Y^N G_{MN}(x, Y(x)) = \tilde{g}_{\mu\nu}(x, Y(x)) - \partial_\mu Y^m \partial_\nu Y^n \tilde{g}'_{mn}(Y(x)). \quad (2)$$

The contribution of branons to the induced metric is then obtained by expanding Equation 2 around the ground state [26, 30, 56]:

$$g_{\mu\nu} = \tilde{g}_{\mu\nu} - \frac{1}{f^4} \delta_{\alpha\beta} \partial_\mu \pi^\alpha \partial_\nu \pi^\beta + \frac{1}{4f^4} \tilde{g}_{\mu\nu} M_{\alpha\beta}^2 \pi^\alpha \pi^\beta + \dots \quad (3)$$

Branons are the mass eigenstates of the brane fluctuations in the extra-space directions. The branon mass matrix $M_{\alpha\beta}$ is determined by the metric properties of the bulk space and, in the absence of a general model for the bulk dynamics, we will consider its elements as free parameters (for an explicit construction see Refs. [57]). Therefore, branons are massless only in highly symmetric cases [26, 30, 56, 58].

Since branon fields survive in the limit in which gravity decouples, $M_D \rightarrow \infty$, branon effects can be studied independent of gravity [59]. We will work in the thin brane limit and assume that the brane dynamics can be described by a low-energy effective action derived from the Nambu-Goto action [26]. Also, branon couplings to the SM fields can be obtained from the SM action defined on a curved background given by the induced metric Equation 2, and expanding in branon fields. Thus the complete action, up to second order in π fields, contains the SM terms, the kinetic term for the branons and the interaction terms between the SM particles and the branons [25, 26, 30, 56].

It is interesting to note that under a parity transformation on the brane, the branon field changes sign if the number of spatial dimensions of the brane is odd, whereas it remains unchanged for even dimensions. Accordingly, branons on a 3-brane are pseudoscalar particles. This fact, in addition to the geometrical origin of the action, implies that terms in the effective Lagrangian with an odd number of branons are forbidden. It means that branons are stable. Strictly speaking, this argument only ensures the stability of the lightest branon ($\tilde{\pi}^1$), the rest of branons can decay to the lightest one, producing SM particles. These decays are very suppressed if the branon spectrum is very degenerate.

In order to analyze such properties we will study the simplest model containing an unstable branon. We consider a model where we have two branons, implying that the number of

extra dimensions has to be two or greater: the lightest one is defined as $\tilde{\pi}^l$, and the heaviest one as $\tilde{\pi}^h$. We will assume very similar masses for them: $\Delta M \equiv M_{\tilde{\pi}^h} - M_{\tilde{\pi}^l} \ll M \simeq M_{\tilde{\pi}^h} \simeq M_{\tilde{\pi}^l}$. Using these energy eigenstates, the SM-branon low-energy effective Lagrangian may be written as [25, 26, 30, 56]:

$$\mathcal{L}_{\tilde{\pi}-\phi} = \frac{I_{\alpha\beta}^\phi}{8f^4} (4\partial_\mu \tilde{\pi}^\alpha \partial_\nu \tilde{\pi}^\beta - M^2 \tilde{\pi}^\alpha \tilde{\pi}^\beta g_{\mu\nu}) T_\phi^{\mu\nu}. \quad (4)$$

Here $\alpha(\beta) = h, l$, and $T_\phi^{\mu\nu}$ is the standard energy-momentum tensor of the particle ϕ evaluated in the background metric:

$$T_\phi^{\mu\nu} = - \left(\tilde{g}^{\mu\nu} \mathcal{L}_\phi + 2 \frac{\delta \mathcal{L}_\phi}{\delta \tilde{g}_{\mu\nu}} \right). \quad (5)$$

The mass matrix is diagonal with eigenvalues $M_{\tilde{\pi}^h} \simeq M_{\tilde{\pi}^l} \simeq M$, whereas the interaction matrix, $I_{\alpha\beta}$, is exactly the identity at first order [25, 26, 30, 56]. However, radiative corrections and higher order terms have a different effect on the interaction eigenstates relative to the energy eigenstates, resulting in suppressed but non-zero cross interaction parameters, λ_ϕ ,

$$I_{\alpha\beta}^\phi \simeq \begin{pmatrix} 1 & \lambda_\phi/2 \\ \lambda_\phi/2 & 1 \end{pmatrix}. \quad (6)$$

This implies that, typically, $\lambda_\phi \sim 0.01$. For simplicity, we will take this parameter to be independent of the particular SM particle, i.e. $\lambda_\phi \simeq \lambda$ for any ϕ . The main conclusions of this paper do not depend on this assumption, although it does introduce an uncertainty of order one for a particular λ_ϕ . However, for the most part of branon phenomenology, both this parameter and ΔM are negligible. General constraints on the branon parameter space we consider are shown in Figure 1: the constraints include those from HERA, Tevatron, and LEP-II (additional bounds from astrophysics and cosmology can be found in [60]).

Thus λ is fundamental to analyze the stability of the heaviest branon. Indeed, if λ is exactly zero, $\tilde{\pi}^h$ is completely stable. If λ is non zero, the heaviest branon decays to the lightest branon and a Standard Model particle anti-particle pair. For the analysis below, we are interested in $\Delta M < 10 \text{ MeV}$, which means that the only available decay channels are $\Gamma_{e^+} : \tilde{\pi}^h \rightarrow \tilde{\pi}^l e^+ e^-$, $\Gamma_\gamma : \tilde{\pi}^h \rightarrow \tilde{\pi}^l \gamma \gamma$, and $\Gamma_\nu : \tilde{\pi}^h \rightarrow \tilde{\pi}^l \nu \bar{\nu}$.

B. Thermal abundances

Branons thus interact in pairs with the SM particles, and the lightest is necessarily stable. In addition, their couplings are suppressed by the brane tension f^4 , which means that they could be in general weakly interacting and massive. As a consequence their freeze-out temperature can be relatively high, which implies that their relic abundance can be cosmologically significant.

In order to calculate the thermal relic branon abundance, the standard techniques have been used in the case of non-relativistic branons at decoupling [33, 60]. The evolution of the number density n_α of branons interacting with SM particles in an expanding Universe is given by the Boltzmann equation:

$$\frac{dn_\alpha}{dt} = -3Hn_\alpha - \langle \sigma_{AV} \rangle (n_\alpha^2 - (n_\alpha^{eq})^2) \quad (7)$$

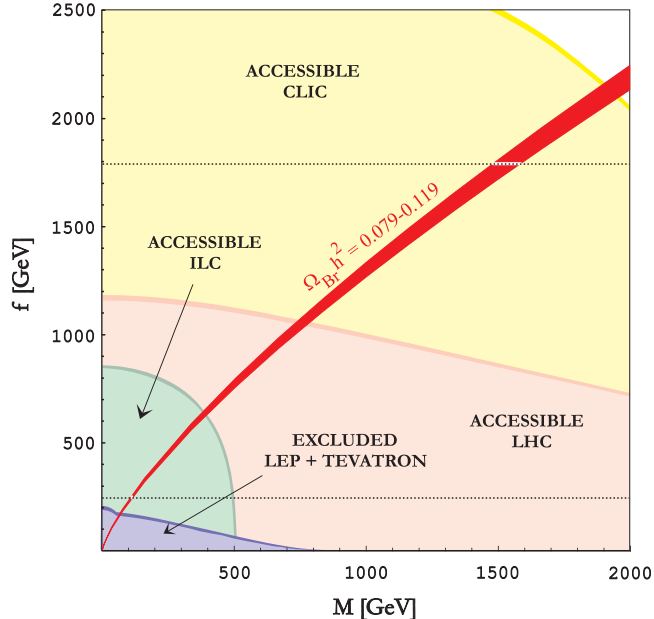


FIG. 1: The relic branon abundance for $N = 2$ in the $f - M$ plane (see Refs. [33, 60] for details). The lower area is excluded by single-photon processes at LEP-II [30, 62] together with monojet signals at Tevatron-I [63]. Prospects for real branon production at future colliders are also shown (See Refs. [30, 63]). The region between the two horizontal dotted lines are preferred by the muon anomalous magnetic moment and electroweak precision observables [28, 61].

where

$$\sigma_A = \sum_X \sigma(\pi^\alpha \pi^\alpha \rightarrow X) \quad (8)$$

is the total annihilation cross section of branons into SM particles X summed over final states. The $-3Hn_\alpha$ term, with H the Hubble parameter, takes into account the dilution of the number density due to the expansion of the Universe. This is the dominant mechanism that sets the total number density of branons. In the scenario we are interested in, the heaviest branon will also decay to the lightest branon, however this effect is insignificant in changing their respective number densities because we focus on lifetimes longer than the age of the Universe. Therefore, the relic density is determined only by the parameters M and f . Each branon species evolves independently and has exactly the same abundance before the decays are effective.

The relic abundance results for two branons of mass M are shown in Figure 1. As expected, for f and M scales of ~ 100 GeV – 1 TeV, we have the correct amount of total non-baryonic dark matter abundance. As shown, these scales are not only in the natural region of parameter space, they are also in the favored region for Brookhaven determinations of the muon anomalous magnetic moment [28, 61].

C. Branon decays

As we have seen, decays of very degenerate branons can be described at low energies by an effective action that depends on four parameters: the branon mass M , the mass splitting ΔM , the cross interaction parameter λ , and the brane tension scale f , which suppresses the coupling of these new particles with the SM. We now determine the decay widths to the relevant SM particles.

Since branons couple directly to the energy momentum tensor, they do not couple directly to a single photon, and thus decays into two-body final states that include a single photon are forbidden. Indeed, this is a general property of scalar or pseudo-scalar particles; the decay of a spin-zero particle into another spin-zero particle and a photon is forbidden by angular momentum conservation. On similar grounds, the decay of a spin-zero particle into another spin-zero particle and a fermion is forbidden. Therefore, unless another light spin-zero particle is added to the Standard Model, the decays of degenerate scalar multiplets will proceed predominantly into three-body final states.

We focus specifically on the limit $M \gg \Delta M$. In this limit, the decay widths can be calculated from Equation 4, the branon Feynman rules given in Ref. [30], and substituting $\delta_{\alpha\beta}$ for $I_{\alpha\beta}$. For photons, we get a differential decay width of

$$\frac{d\Gamma_\gamma(\varepsilon_\gamma)}{d\varepsilon_\gamma} = \frac{\lambda^2 \varepsilon_\gamma^3 (\Delta M - \varepsilon_\gamma)^3 M^2}{24 f^8 \pi^3}, \quad (9)$$

which implies a total photon decay width of

$$\Gamma_\gamma = \left[1.67 \times 10^{20} s. \left[\frac{10^{-2}}{2\lambda} \right]^2 \left[\frac{f}{M} \right]^2 \left[\frac{4 \text{ MeV}}{\Delta M} \right]^7 \left[\frac{f}{1 \text{ TeV}} \right]^6 \right]^{-1}. \quad (10)$$

If $\Delta M > 2m_e$, the heaviest branon can also decay to the lightest one and an electron-positron pair. The spectrum of the outgoing positron in the same limit of $M \gg \Delta M$ is:

$$\begin{aligned} \frac{d\Gamma_{e^+}(\varepsilon_{e^+}, m_e)}{d\varepsilon_{e^+}} &= \frac{\lambda^2 M^2}{2 f^8 (4\pi)^3} \sqrt{(\varepsilon_{e^+}^2 - m_e^2)((\Delta M - \varepsilon_{e^+})^2 - m_e^2)} \\ &\quad \left\{ 4(\Delta M - 2\varepsilon_{e^+})^2 [(\Delta M - \varepsilon_{e^+})\varepsilon_{e^+} - 16m_e^2] \right. \\ &\quad \left. + m_e^2 [225(\Delta M - \varepsilon_{e^+})\varepsilon_{e^+} - 177m_e^2] \right\}. \end{aligned} \quad (11)$$

The kinematic limits for the total energy of the outgoing positron are $m_e > \varepsilon_{e^+} > \Delta M - m_e$.

Finally, we note that in the kinematic limits we study it is also possible to produce neutrinos:

$$\frac{d\Gamma_{\nu_i}(\varepsilon_{\nu_i})}{d\varepsilon_{\nu_i}} = \frac{1}{2} \frac{d\Gamma_{e^+}(\varepsilon_{\nu_i}, 0)}{d\varepsilon_{\nu_i}}, \quad (12)$$

where i labels the species of neutrino (we have neglected the neutrino mass). Since diffuse neutrino bounds are much weaker than diffuse photon bounds at MeV energies, there are likely minimal phenomenological implications of neutrino production in this model (see Refs. [64, 65] for recent determinations of neutrino constraints of annihilating and decaying dark matter models). The decay widths for all of these channels are shown in Figure 2.

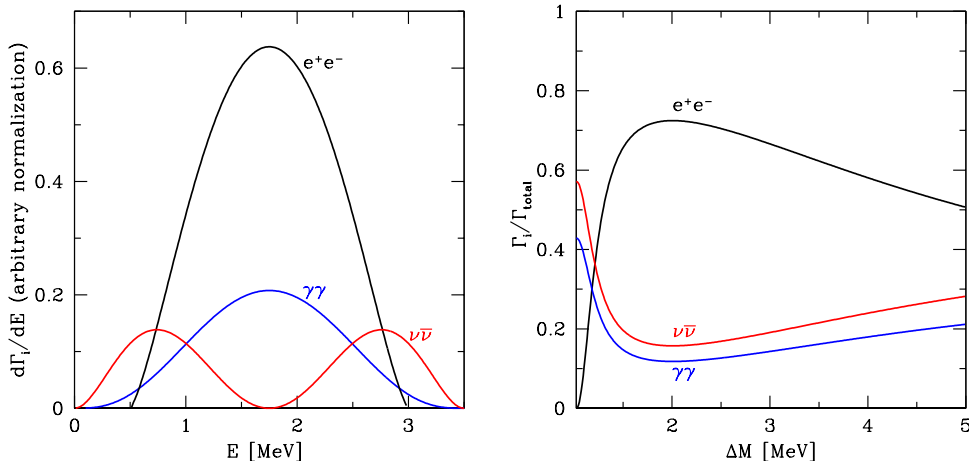


FIG. 2: *Left*: The differential decay widths for $\tilde{\pi}^h \rightarrow \tilde{\pi}^l e^+ e^-$, $\tilde{\pi}^l \gamma \gamma$, and $\tilde{\pi}^l \nu \bar{\nu}$, assuming $\Delta M = 3.5$ MeV. *Right*: The total branching fraction for each case as a function of ΔM . In both figures, for $\nu \bar{\nu}$, we have accounted for the decays to all three species of neutrinos.

IV. GALACTIC AND EXTRAGALACTIC SIGNALS

We now determine the extragalactic and Galactic gamma-ray signals from the decays of unstable $\tilde{\pi}^h$'s. Although the resulting fluxes of course depend on the specific model parameters and couplings, the formalism we present here can be used for any similar model that decays via three-body final states. In what follows, the mass of the NLP is defined as M , the mass splitting between the NLP and LP is ΔM , and the lifetime of the NLP into a given branching ratio, ι , as $1/\tau^\iota = \Gamma_\iota = \int dE d\Gamma_\iota/dE$.

A. Galactic 511 keV flux

We begin by considering the 511 keV line emission resulting from positron injection in the Galactic bulge. Given the small propagation distance of the positrons as described above, we assume that the location of the $e^+ e^-$ annihilation and 511 keV photon creation faithfully tracks the dark matter halo distribution. Defining s as the distance from the Sun to any point in the halo, Ψ as the angle between the Galactic center and any point in the halo, and $D = 8.5$ kpc as the distance from the Sun to the Galactic center, the 511 keV line intensity from decays is

$$\frac{d\Phi_{511}(\Psi)}{d\Omega} = \frac{1}{4\pi} \int_0^\infty \frac{dn_{511}[r(s, \Psi)]}{dt} ds, \quad (13)$$

where $r^2(s, \Psi) = D^2 + s^2 - 2Ds \cos \Psi$, and the solid angle is defined as $\Delta\Omega = 2\pi(1 - \cos \Psi)$. The number density of dark matter particles is $\rho(r)/M$, where $\rho(r)$ is the density of dark matter in the halo of the Milky Way, which we assume to be spherically symmetric. Consequently, the total number of 511 keV photons produced per unit time can be estimated as $dn_{511}/dt = 2(1 - 3p/4)n_{\tilde{\pi}^h}\Gamma_{e^+} = (1 - 3p/4)\rho\Gamma_{e^+}/M$, where we are assuming that $\tilde{\pi}^h$ accounts for half of the dark matter (the other half is in form of $\tilde{\pi}^l$), that the positrons are stopped before annihilation, and that this annihilation takes place through positronium

formation p fraction of the time. As we have discussed above, $p \simeq 0.94$.

Both the total flux within the field-of-view and the angular distribution of the flux depend crucially on the shape of the dark matter density profile. Numerical simulations with only dark matter have shown that the halos consisting of cold dark matter particles have a Navarro-Frenk-White (NFW) type density profile, $\rho(r) = \rho_0/(r/r_0)/(1+r/r_0)^2$, where ρ_0 is the scale density and r_0 is the scale radius [66]. The NFW profile, however, does not account for the effect of baryonic physics, which is expected to be important in setting the central density of Milky Way-type galaxies, due to the relatively large baryonic contribution in the central regions. A full understanding of the halo density profile must adequately account for the energy exchange processes between the baryons and dark matter, which is currently lacking. These interactions are particularly important in the interior regions, and it is currently not understood if these interactions steepen the central density of the dark matter halo or flatten it out. From an observational perspective, there is also a wide uncertainty in the density profile and mass model of the Milky Way halo. For example, Ref. [67] argues that the large number of microlensing constraints towards the Galactic bulge is inconsistent with central slopes steeper than $r^{-0.4}$. Ref. [68] apply a variety of observational constraints to an adiabatically-contracted NFW model, and find that NFW-like central slopes provide an excellent fit to the data.

To allow for the greatest flexibility, we model the density profile of the Milky Way in the form of

$$\rho(r) = \frac{\rho_0}{(r/r_0)^\gamma [1 + (r/r_0)^\alpha]^{(\beta-\gamma)/\alpha}}, \quad (14)$$

where ρ_0 is the scale radius, r_0 is the scale density. The combination of γ and β set the inner and outer slopes of the halo profile, respectively, while α controls the sharpness of the transition between the inner and outer slopes. We determine the shape parameters α , β , and γ , as well as the normalization parameters ρ_0 and r_0 by fitting to both the angular distribution of the INTEGRAL signal and the constraints on the Milky Way halo. The parameters ρ_0 and γ are primarily determined by the INTEGRAL data, whereas the remaining parameters are fixed by the total mass and local density of the dark matter halo. The intensity of the INTEGRAL signal is so low at high longitudes that it is difficult to discriminate from the instrumental background, and thus fix the parameters that do not directly effect the central region of the halo.

In Figure 3, we show an example halo profile that fits the angular distribution of the 511 keV intensity, and is normalized to match the total flux of $1.05 \times 10^{-3} \text{ cm}^{-2} \text{ s}^{-1}$ within the Galactic bulge. For simplicity, we assume that the 511 keV emission is entirely a result of dark matter decays, and does not include any contribution from sources discussed above, such as SNIa. Here we use $\Delta M = 3.5 \text{ MeV}$, $M_{\tilde{\pi}^h} = 700 \text{ GeV}$, $\lambda = 0.0085$, and a brane tension of $f = 1 \text{ TeV}$; these model parameters naturally give the correct relic dark matter abundance, as seen in Figure 1. The implied parameters describing the halo model are $\rho_0 = 0.12 \text{ GeV cm}^{-3}$, $r_0 = 10 \text{ kpc}$, $\gamma = 1.5$, $\beta = 3$, $\alpha = 8$. With these halo model parameters, the total dark matter halo mass is in accord, to within statistical uncertainties, with the mass determinations from the kinematics of satellite galaxies [69, 70]. In addition to the true signal, which is shown as a solid line in Figure 3, we show two curves with angular resolutions of 1° and 3° ; these are similar to the $\sim 3^\circ$ FWHM angular resolution of SPI.

In Figure 3, we have focused on matching the normalization and angular distribution of the flux within the Galactic center region, where the 511 keV flux is well-determined. As an additional check on the viability of the model, we must be sure not to overproduce

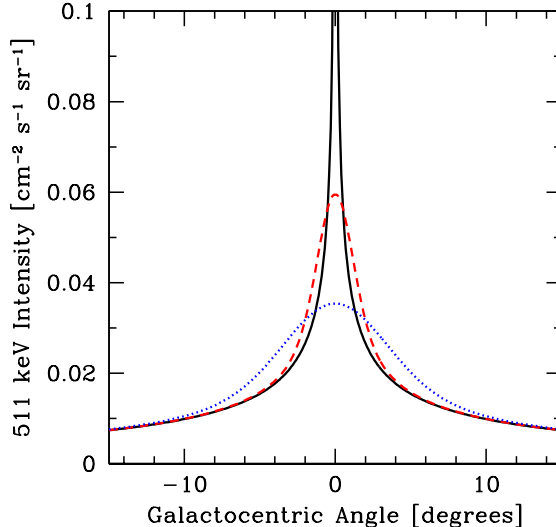


FIG. 3: The 511 keV intensity from the decays of unstable $\tilde{\pi}^h$'s as a function of Galactocentric angle. The intensity has been normalized to the total flux of $1.05 \times 10^{-3} \text{ cm}^{-2} \text{ s}^{-1}$ within the Galactic bulge, and the dark matter halo is described by Equation 14 with $\alpha = 8$, $\beta = 3$, and $\gamma = 1.5$. The solid (black) line is the true signal, the dashed (red) line is the signal smoothed with a 1° angular resolution, and the dotted (blue) curve is for a 3° angular resolution. We have used a positronium fraction $p = 0.94$, and the branon model parameters $\Delta M = 3.5 \text{ MeV}$, $f = 1 \text{ TeV}$, and $M_{\tilde{\pi}^h} = 700 \text{ GeV}$. The angular distribution of the INTEGRAL signal is spherically-symmetric about the Galactic bulge, with a FWHM of 8° .

the observed 511 keV emission from high longitudes in the Galactic disk. We can examine constraints on a potential high longitude disk flux by separately considering both emission from the Galactic center region and large-scale extended diffuse emission. Regarding the Galactic center region emission, we use the most recent INTEGRAL results, which shows that the 511 keV bulge-to-disk flux ratio is $\sim 1-3$ and that the intensity is reduced by a factor ~ 6 at latitudes and longitudes of 10° relative to the Galactic center [34]. As seen in Figure 3, the chosen profile satisfies these constraints. Regarding the large scale ($\gtrsim 20^\circ$) diffuse 511 keV emission, we consider the results of Ref. [71]. Using the INTEGRAL effective area of 75 cm^2 at 511 keV, and smoothing the solid curve in Figure 3 with a gaussian comparable to the $\sim 20^\circ$ FWHM spatial scales resolved in Ref. [71], we find a 511 keV rate of $\sim 0.06 \text{ s}^{-1}$ at $l = 0^\circ$, and $\sim 0.01 \text{ s}^{-1}$ at $l = 30^\circ$. These rates were determined by subtracting the flux at $b = 20^\circ$, and are consistent with the rates determined in Ref. [71]. Thus we find that the halo profile used in Figure 3 is consistent with 511 keV emission constraints at high Galactic longitude.

Before moving on to consider the direct production of gamma-rays in $\tilde{\pi}^h$ decays, we make one additional comment regarding the assumed value of the positronium fraction. Motivated by the detailed fits by INTEGRAL, for all of the above results we have taken the positronium fraction to be $p = 0.94$. However, the precise determination of p is model dependent, as discussed above. If the decays we consider do indeed account for a large fraction of the 511 keV signal, a redetermination of p will be required by explicitly fitting both the Galactic and extragalactic fluxes. Inclusion of the latter flux will be important, even in the direction of the Galactic center, given that the extragalactic and Galactic fluxes are similar to within an order of magnitude, depending specifically on the shape of the halo model. The similarity

of extragalactic and Galactic fluxes is unique to the models we consider; in the case of dark matter annihilation, for example, the extragalactic flux is typically several orders of magnitude below the flux from any direction in the Galaxy itself.

B. High latitude gamma-ray flux

We now turn to determining the contribution to the high latitude iDPB from three-body decays to gamma-rays, both from the Galactic halo and from extragalactic sources. First considering extragalactic sources, these decays will be visible only if they occur in the late Universe, in the matter or vacuum dominated eras. Assuming a smooth distribution of dark matter in the Universe (modifications to this assumption will be discussed below), the differential gamma-ray flux from a general three-body decay is

$$\frac{d\Phi}{dE_\gamma} = \frac{n_\gamma}{4\pi} \int_0^{t_0} dt \frac{N(t)}{a V_0} \frac{d\Gamma_\gamma}{d\varepsilon_\gamma}. \quad (15)$$

Here n_γ is the number of photons produced in a single decay; a is the scale factor of the Universe; $t_0 \simeq 4.3 \times 10^{17}$ s is the age of the Universe; $N(t) = N^{\text{in}} e^{-t/\tau}$, where N^{in} is the number of decaying particles at freeze-out; and V_0 is the present volume of the Universe. The relation between the produced energy, ε_γ , and observed energy, E_γ , is given by $d\varepsilon_\gamma/dE_\gamma = (1+z) \equiv a^{-1}$. In Equation 15, we have assumed that gamma-rays do not get attenuated on cosmological gamma-ray backgrounds from their redshift of production. We find this to be an excellent approximation over the energies and redshifts we are considering [72]. In the BWS, $n_\gamma = 2$, however this factor gets cancelled because 1/2 of the dark matter consists of unstable $\tilde{\pi}^{\text{h}}$'s.

We are interested in decays such that $\tau \gg t_0$. In this case, we can write $t \simeq P(a)$, where

$$P(a) \equiv \frac{2 \left(\ln \left[\sqrt{\Omega_\Lambda a^3} + \sqrt{\Omega_M + \Omega_\Lambda a^3} \right] - \ln \left[\sqrt{\Omega_M} \right] \right)}{3H_0 \sqrt{\Omega_\Lambda}}. \quad (16)$$

The differential photon flux coming from the decays may be written as

$$\frac{d\Phi}{dE_\gamma} \simeq \frac{n_\gamma N^{\text{in}}}{4\pi V_0} \int_{E_\gamma/\Delta M}^1 da \frac{e^{-P(a)/\tau}}{aQ(a)} \frac{d\Gamma_\gamma}{d\varepsilon_\gamma} \Big|_{\varepsilon_\gamma=E_\gamma/a}, \quad (17)$$

where we have defined

$$\frac{da}{dt} = aH \simeq H_0 \sqrt{\frac{\Omega_M}{a} + \Omega_\Lambda a^2} \equiv Q(a). \quad (18)$$

For lifetimes much longer than the age of the Universe, the exponential factor in Equation 17 is negligible. We neglect the radiation content, $\Omega_R \sim 0$, as well as the curvature term, $k \sim 0$. Though the extragalactic flux is dependent on cosmological parameters [17], here we choose to fix the parameters to match the observed concordance cosmological model [73].

The high latitude iDPB also receives a significant contribution from decays in the halo of the Galaxy. The flux from Galactic halo dark matter decays directly into photons can also be calculated using Equation 13, accounting for the fact that the flux comes from high latitudes, $\gtrsim 10^\circ$, and averaging the flux over a $\sim 10^{-3}$ sr field of view. This latter quantity corresponds

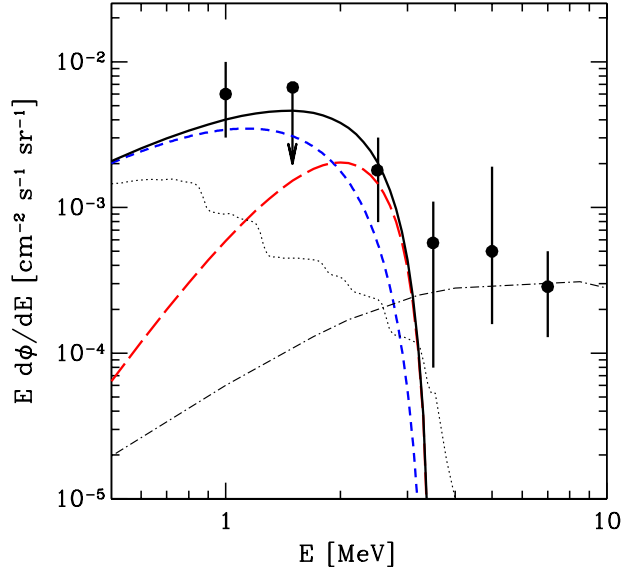


FIG. 4: The high latitude isotropic diffuse photon background in the MeV regime, as measured by COMPTEL (circles) [43]. The short-dashed curve is the contribution from extragalactic decays, the long-dashed curve is the contribution from decays in the Galactic halo, and the solid curve is the sum of both extragalactic and Galactic contributions. The branon model parameters are the same as those in Figure 3. Two additional standard contributions to the iDPB are shown: Type Ia Supernovae (SNIa; dotted) and blazars (dot-dashed). The blazar background has been normalized to the gamma-ray background at energies $\gtrsim 10$ MeV [49], while the normalization of the SNIa spectrum is taken from Ref. [50].

to the field of view characteristic of MeV gamma-ray instruments such as COMPTEL. With BWS parameters fixed by the 511 keV signal, in Figure 4 we show the contribution to the iDPB from high latitude Galactic and extragalactic $\tilde{\pi}^h$ decays. Again, unstable $\tilde{\pi}^h$'s account for 1/2 of the relic abundance of dark matter. In the calculation of the observed spectrum, we have not accounted for finite detector energy resolution; including these effects will likely further smooth out the endpoints of the spectrum, and bring the shape of the spectrum into even better agreement with the approximate power-law spectrum observed by COMPTEL.

V. DISCUSSION

Above we have shown that, assuming both an abundance of non-baryonic dark matter that matches cosmological observations and WIMP scale masses, within the BWS two parameters are required to independently match the 511 keV line flux and the \sim MeV iDPB. We now discuss independent constraints on this model as well as potential implications of these results.

A. Gamma-rays from the Galactic center

In section IV we have focused on the high latitude Galactic gamma-ray background. There will additionally of course be a significant contribution to the low-latitude gamma-ray background from $\tilde{\pi}^h$ decays, in particular in the direction the Galactic center. We must

be sure that the model parameters we consider above do not violate the COMPTEL flux measurements in this direction.

We can make a simple estimate of the gamma-ray flux in the direction of the Galactic center by considering the branching ratios determined in section III. Using these branching ratios, in combination with the number of gamma-rays produced per e^+e^- annihilation (section II), the ratio of the total number of photons produced at 511 keV to the total number of photons produced directly in the two photon decays for our model parameters is simply

$$\frac{\Gamma_e}{\Gamma_\gamma} \left(1 - \frac{3}{4}p\right) \simeq 0.9. \quad (19)$$

In general, we can expect a ratio of order one for any model that has similar branching ratios to photons and positrons. Thus we expect a continuous gamma-ray flux $\lesssim 10^{-2} \text{ cm}^{-2} \text{ s}^{-1} \text{ sr}^{-1}$ at $\sim \text{MeV}$ energies from the Galactic center. Interestingly, COMPTEL has measured a diffuse flux from the Galactic center at this order of magnitude in the energy range 1–3 MeV [55]. The COMPTEL flux is seen to vary slowly with energy, and is reduced by a factor ~ 2 at a Galactic latitude of $\sim 10^\circ$. We find that, for the dark matter halo profile considered above, the diffuse MeV gamma-ray emission from $\tilde{\pi}^h$ decays is consistent with the COMPTEL flux both at the Galactic center and at higher latitudes. Since, as discussed above, the source of MeV gamma-rays from the Galactic center is uncertain, it is interesting to consider dark matter decays as the source of this emission.

In addition to the diffuse Galactic gamma-rays, INTEGRAL has placed strong constraints on the presence of anomalous gamma-ray lines in the energy regimes $\sim 10 - 8000 \text{ keV}$ within 13° from the Galactic center [71]. For example, at energies $\sim \text{MeV}$, lines of width $\sim \text{keV}$ are constrained to have a flux $\lesssim 10^{-4} \text{ cm}^{-2} \text{ s}^{-1}$, and “lines” of width $\sim \text{MeV}$ are constrained to have a flux $\lesssim 10^{-3} \text{ cm}^{-2} \text{ s}^{-1}$. Given the width of the gamma-ray spectra we consider (see Figure 2), the latter flux limits are relevant for $\tilde{\pi}^h$ decays. As a result, the INTEGRAL line constraints are no more stringent than the COMPTEL constraints on diffuse MeV gamma-ray emission.

B. Assumption of smooth halo and angular distribution

The extragalactic flux from dark matter decays depends on the distribution of dark matter halos in the Universe, while the Galactic flux depends on the distribution of dark matter within the Milky Way halo. In principle, both of these fluxes also depend on the presence of “substructure” within dark matter halos [74]. While we have assumed that the distribution of dark matter is smooth both in the Universe and in the Galactic halo, we can gain some insight as to the effects of clumping by considering the simplifying limit in which all of the substructures are at a common mass, the internal density of the substructures is constant, and the radial distribution of substructures in the halo follows the same density profile as the smooth dark matter halo. In reality, it is likely that the two radial distributions differ, which may affect our simple estimate. Under these assumptions, we find that, in a given direction, the increase in the flux over the smooth halo is simply $1 + f$, where f is the fraction of the halo contained in substructures. Typically, $f \simeq 0.01$ [74]. This small increase simply quantifies the probability that any one of these substructures is within a given field of view.

Regarding the determination of the extragalactic gamma-ray flux from $\tilde{\pi}^h$ decays, we have assumed a smooth distribution of $\tilde{\pi}^h$'s in the Universe, and have neglected the clumping in

dark matter halos. Given the above considerations, the clumping in halos will likely have minimal effect on the mean flux signal, though the situation will be different when considering the angular distribution of gamma-rays. The angular distribution depends not only on the parameters describing the branon model, but also on the cosmological evolution of dark matter halos as a function of redshift. Similar to the case of standard annihilating neutralino WIMP dark matter, the angular distribution of gamma-rays from decays is expected to be distinct from astrophysical sources such as AGN and supernovae, and may provide a way to discriminate between the sources of the iDPB [75, 76]. We consider this analysis in a forthcoming study.

VI. CONCLUSIONS

In this paper, we have analyzed the general possibility that decaying dark matter may be the source of both the 511 keV gamma-ray line from the Galactic center and the diffuse high latitude photon background at energies between 1 and 5 MeV. We have introduced a new scenario where a dark matter particle is nearly degenerate with a lighter daughter, with mass splitting \sim MeV and lifetime $\sim 10^3$ times the present age of the Universe. The decays of the dark matter are into three body final states: a Standard Model particle anti-particle pair and a daughter dark matter particle. Remarkably, we find that the above mass splitting and lifetime are exactly that which is required to explain both of the above gamma-ray emissions, provided there is similar branching ratios to electrons and photons.

We have illustrated this idea with a concrete model of brane-world dark matter, and we have shown that a standard WIMP motivated within the brane-world scenario, the branon, can explain both observations with natural values required to obtain the correct dark matter relic abundance. Using the effective low-energy Lagrangian for a model with two branons interacting with the Standard Model fields, we have computed the decay rates of the heaviest branon into the lighter one and pairs of Standard Model particles, in particular focusing on electron-positron pairs and photons. We find that the branon model not only produces positrons and gamma-rays at the required rates, it also provides unique and novel phenomenology that will be tested by future MeV gamma-ray observatories.

Acknowledgments

We are very grateful to Jonathan Feng, Matt Kistler, and especially John Beacom and Hasan Yuksel for several useful discussions on this paper. The work of JARC is supported in part by DOE grant DOE/DE-FG02-94ER40823, by the FPA 2005-02327 project (DGICYT, Spain) and the McCue Award from the UCI Center for Cosmology. LES acknowledges support from NSF grant AST-0607746.

-
- [1] G. Jungman, M. Kamionkowski, and K. Griest, Phys. Rept. **267**, 195 (1996), hep-ph/9506380.
 - [2] H. Baer and M. Brhlik, Phys. Rev. **D57**, 567 (1998), hep-ph/9706509.
 - [3] L. Bergstrom, Rept. Prog. Phys. **63**, 793 (2000), hep-ph/0002126.
 - [4] H.-C. Cheng, J. L. Feng, and K. T. Matchev, Phys. Rev. Lett. **89**, 211301 (2002), hep-ph/0207125.

- [5] G. Bertone, D. Hooper, and J. Silk, Phys. Rept. **405**, 279 (2005), hep-ph/0404175.
- [6] V. Berezhinsky, M. Kachelriess, and A. Vilenkin, Phys. Rev. Lett. **79**, 4302 (1997), astro-ph/9708217.
- [7] C. Boehm, D. Hooper, J. Silk, M. Casse, and J. Paul, Phys. Rev. Lett. **92**, 101301 (2004), astro-ph/0309686.
- [8] C. Picciotto and M. Pospelov, Physics Letters B **605**, 15 (2005), arXiv:hep-ph/0402178.
- [9] D. Hooper and L.-T. Wang, Phys. Rev. **D70**, 063506 (2004), hep-ph/0402220.
- [10] F. Ferrer and T. Vachaspati, Phys. Rev. Lett. **95**, 261302 (2005), astro-ph/0505063.
- [11] S. Kasuya and M. Kawasaki, Phys. Rev. D **73**, 063007 (2006), arXiv:astro-ph/0602296.
- [12] D. P. Finkbeiner and N. Weiner, Phys. Rev. **D76**, 083519 (2007), astro-ph/0702587.
- [13] M. Pospelov and A. Ritz, Physics Letters B **651**, 208 (2007), arXiv:hep-ph/0703128.
- [14] G. D. Kribs and I. Z. Rothstein, Phys. Rev. **D55**, 4435 (1997), hep-ph/9610468.
- [15] K. Ahn and E. Komatsu, Phys. Rev. D **72**, 061301 (2005), arXiv:astro-ph/0506520.
- [16] K. Lawson and A. R. Zhitnitsky, ArXiv e-prints **704** (2007), 0704.3064.
- [17] J. A. R. Cembranos, J. L. Feng, and L. E. Strigari, Phys. Rev. Lett. **99**, 191301 (2007), arXiv:0704.1658 [astro-ph].
- [18] J. A. R. Cembranos, J. L. Feng, and L. E. Strigari, Phys. Rev. D **75**, 036004 (2007), arXiv:0708.0239.
- [19] H. Yuksel and M. D. Kistler (2007), arXiv:0711.2906 [astro-ph].
- [20] G. Bertone, W. Buchmuller, L. Covi, and A. Ibarra, JCAP **0711**, 003 (2007), arXiv:0709.2299 [astro-ph].
- [21] N. Arkani-Hamed, S. Dimopoulos, and G. R. Dvali, Phys. Lett. **B429**, 263 (1998), hep-ph/9803315.
- [22] I. Antoniadis, N. Arkani-Hamed, S. Dimopoulos, and G. R. Dvali, Phys. Lett. **B436**, 257 (1998), hep-ph/9804398.
- [23] D. Langlois, Prog. Theor. Phys. Suppl. **148**, 181 (2003), hep-th/0209261.
- [24] T. Multamaki and I. Vilja, Phys. Lett. **B559**, 1 (2003), hep-th/0301168.
- [25] R. Sundrum, Phys. Rev. **D59**, 085010 (1999), hep-ph/9807348.
- [26] A. Dobado and A. L. Maroto, Nucl. Phys. **B592**, 203 (2001), hep-ph/0007100.
- [27] M. Bando, T. Kugo, T. Noguchi, and K. Yoshioka, Phys. Rev. Lett. **83**, 3601 (1999), hep-ph/9906549.
- [28] J. A. R. Cembranos, A. Dobado, and A. L. Maroto, Phys. Rev. **D73**, 035008 (2006), hep-ph/0510399.
- [29] P. Creminelli and A. Strumia, Nucl. Phys. **B596**, 125 (2001), hep-ph/0007267.
- [30] J. Alcaraz, J. A. Cembranos, A. Dobado, and A. L. Maroto, Phys. Rev. D **67**, 075010 (2003), arXiv:hep-ph/0212269.
- [31] J. A. R. Cembranos, A. Dobado, and A. L. Maroto, AIP Conf. Proc. **670**, 235 (2003), hep-ph/0301009.
- [32] T. Kugo and K. Yoshioka, Nucl. Phys. **B594**, 301 (2001), hep-ph/9912496.
- [33] J. A. Cembranos, A. Dobado, and A. L. Maroto, Physical Review Letters **90**, 241301 (2003), arXiv:hep-ph/0302041.
- [34] J. Knödseder, P. Jean, V. Lonjou, G. Weidenspointner, N. Guessoum, W. Gillard, G. Skinner, P. von Ballmoos, G. Vedrenne, J.-P. Roques, et al., Astron. Astrophys. **441**, 513 (2005), arXiv:astro-ph/0506026.
- [35] W. N. Johnson, III and R. C. Haymes, Astrophys. J. **184**, 103 (1973).
- [36] J. F. Beacom and H. Yuksel, Phys. Rev. Lett. **97**, 071102 (2006), astro-ph/0512411.

- [37] P. Jean, J. Knödseder, V. Lonjou, M. Allain, J.-P. Roques, G. K. Skinner, B. J. Teegarden, G. Vedrenne, P. von Ballmoos, B. Cordier, et al., *Astron. Astrophys.* **407**, L55 (2003), arXiv:astro-ph/0309484.
- [38] J. F. Beacom, N. F. Bell, and G. Bertone, *Phys. Rev. Lett.* **94**, 171301 (2005), astro-ph/0409403.
- [39] E. Kalemci, S. E. Boggs, P. A. Milne, and S. P. Reynolds, *Astrophys. J.* **640**, L55 (2006), astro-ph/0602233.
- [40] P. A. Sturrock, *Astrophys. J.* **164**, 529 (1971).
- [41] R. Ramaty, B. Kozlovsky, and R. E. Lingenfelter, *Astrophys. J. S.* **40**, 487 (1979).
- [42] B. Kozlovsky, R. E. Lingenfelter, and R. Ramaty, *Astrophys. J.* **316**, 801 (1987).
- [43] G. Weidenspointner, M. Varendorff, S. C. Kappadath, K. Bennett, H. Bloemen, R. Diehl, W. Hermsen, G. G. Lichti, J. Ryan, and V. Schönfelder, in *American Institute of Physics Conference Series*, edited by M. L. McConnell and J. M. Ryan (2000), vol. 510 of *American Institute of Physics Conference Series*, pp. 467–+.
- [44] K. Watanabe, M. D. Leising, G. H. Share, and R. L. Kinzer, in *American Institute of Physics Conference Series*, edited by M. L. McConnell and J. M. Ryan (2000), vol. 510 of *American Institute of Physics Conference Series*, pp. 471–+.
- [45] E. Churazov, R. Sunyaev, M. Revnivtsev, S. Sazonov, S. Molkov, S. Grebenev, C. Winkler, A. Parmar, A. Bazzano, M. Falanga, et al., *Astron. Astrophys.* **467**, 529 (2007), arXiv:astro-ph/0608250.
- [46] Y. Ueda, M. Akiyama, K. Ohta, and T. Miyaji, *Astrophys. J.* **598**, 886 (2003), arXiv:astro-ph/0308140.
- [47] V. Pavlidou and B. D. Fields, *Astrophys. J. Lett.* **575**, L5 (2002), arXiv:astro-ph/0207253.
- [48] A. Loeb and E. Waxman, *Nature* **405**, 156 (2000), arXiv:astro-ph/0003447.
- [49] K. McNaron-Brown, W. N. Johnson, G. V. Jung, R. L. Kinzer, J. D. Kurfess, M. S. Strickman, C. D. Dermer, D. A. Grabelsky, W. R. Purcell, M. P. Ulmer, et al., *Astrophys. J.* **451**, 575 (1995).
- [50] L. E. Strigari, J. F. Beacom, T. P. Walker, and P. Zhang, *Journal of Cosmology and Astroparticle Physics* **4**, 17 (2005), arXiv:astro-ph/0502150.
- [51] K. Ahn, E. Komatsu, and P. Höflich, *Phys. Rev. D* **71**, 121301 (2005), arXiv:astro-ph/0506126.
- [52] P.-J. Zhang and J. F. Beacom, *Astrophys. J.* **614**, 37 (2004), astro-ph/0401351.
- [53] W. A. Strong, H. Bloemen, R. Diehl, W. Hermsen, and V. Schönfelder, *Astrophysical Letters Communications* **39**, 209 (1999), arXiv:astro-ph/9811211.
- [54] F. Lebrun, R. Terrier, A. Bazzano, G. Bélanger, A. Bird, L. Bouchet, A. Dean, M. Del Santo, A. Goldwurm, N. Lund, et al., *Nature (London)* **428**, 293 (2004).
- [55] A. W. Strong, I. V. Moskalenko, and O. Reimer, *Astrophys. J.* **537**, 763 (2000), arXiv:astro-ph/9811296.
- [56] J. A. Cembranos, A. Dobado, and A. L. Maroto, *Phys. Rev. D* **65**, 026005 (2002), arXiv:hep-ph/0106322.
- [57] A. A. Andrianov, V. A. Andrianov, P. Giacconi, and R. Soldati, *JHEP* **07**, 063 (2003), hep-ph/0305271.
- [58] J. A. R. Cembranos, A. Dobado, and A. L. Maroto, *Int. J. Mod. Phys. D* **13**, 2275 (2004), hep-ph/0405165.
- [59] R. Contino, L. Pilo, R. Rattazzi, and A. Strumia, *JHEP* **06**, 005 (2001), hep-ph/0103104.
- [60] J. A. Cembranos, A. Dobado, and A. L. Maroto, *Phys. Rev. D* **68**, 103505 (2003), arXiv:hep-

- ph/0307062.
- [61] J. A. R. Cembranos, A. Dobado, and A. L. Maroto, *Phys. Rev.* **D73**, 057303 (2006), hep-ph/0507066.
 - [62] P. Achard et al. (L3), *Phys. Lett.* **B597**, 145 (2004), hep-ex/0407017.
 - [63] J. A. R. Cembranos, A. Dobado, and A. L. Maroto, *Phys. Rev.* **D70**, 096001 (2004), hep-ph/0405286.
 - [64] H. Yuksel, S. Horiuchi, J. F. Beacom, and S. Ando (2007), arXiv:0707.0196 [astro-ph].
 - [65] S. Palomares-Ruiz (2007), arXiv:0712.1937 [astro-ph].
 - [66] J. F. Navarro, C. S. Frenk, and S. D. M. White, *Astrophys. J.* **490**, 493 (1997), astro-ph/9611107.
 - [67] J. J. Binney and N. W. Evans, *Mon. Not. Roy. Astron. Soc.* **327**, L27 (2001), astro-ph/0108505.
 - [68] A. Klypin, H. Zhao, and R. S. Somerville, *Astrophys. J.* **573**, 597 (2002), astro-ph/0110390.
 - [69] M. I. Wilkinson and N. W. Evans, *Mon. Not. Roy. Astron. Soc.* **310**, 645 (1999), astro-ph/9906197.
 - [70] T. Sakamoto, M. Chiba, and T. C. Beers, *Astron. Astrophys.* **397**, 899 (2003), astro-ph/0210508.
 - [71] B. J. Teegarden and K. Watanabe, *Astrophys. J.* **646**, 965 (2006), arXiv:astro-ph/0604277.
 - [72] X.-L. Chen and M. Kamionkowski, *Phys. Rev.* **D70**, 043502 (2004), astro-ph/0310473.
 - [73] D. N. Spergel et al. (WMAP), *Astrophys. J. Suppl.* **170**, 377 (2007), astro-ph/0603449.
 - [74] J. Diemand, M. Kuhlen, and P. Madau, *Astrophys. J.* **657**, 262 (2007), astro-ph/0611370.
 - [75] P. Ullio, L. Bergstrom, J. Edsjo, and C. G. Lacey, *Phys. Rev.* **D66**, 123502 (2002), astro-ph/0207125.
 - [76] S. Ando, E. Komatsu, T. Narumoto, and T. Totani, *Phys. Rev.* **D75**, 063519 (2007), astro-ph/0612467.